

# Chapter 7

## Causes and Impacts of Coastal Inundation



Lynn Donelson Wright, Donald T. Resio and C. Reid Nichols

*You never really know what's coming. A small wave, or maybe a big one. All you can really do is hope that when it comes, you can surf over it, instead of drown in its monstrosity.*

— Alysha Speer

### 7.1 Rising Damp: Many Causes

According to NOAA's Office of Coastal Management, inundation events are the dominant causes of natural-hazard-related deaths in the U.S. and are also the most frequent and costly of the natural hazards affecting the nation. The effects of inundation in other nations such as Bangladesh, Indonesia, Thailand and India are often devastating. While the long-term rises in mean sea level as discussed in Part 1, Chap. 3 are instrumental in allowing inundation to reach farther inland and to ever higher elevations, it is the short-lived episodic, non-tidal, events that cause the most damage. Included among these inundation causes are tsunamis, storm surges, coastal flooding caused by onshore winds and wave-induced set up, river and inland flooding and extreme rainfall events. The deepest flooding occurs when two or more of these phenomena reinforce each other and coincide with perigean spring high tides (aka. "king tides"). For example, it is common for tropical cyclones to

---

L. D. Wright (✉)

Southeastern Universities Research Association (SURA), Washington, DC, USA  
e-mail: ldwright@bellsouth.net

D. T. Resio

School of Engineering, University of North Florida, Jacksonville, FL, USA  
e-mail: don.resio@unf.edu

C. R. Nichols

Marine Information Resources Corporation (MIRC), Ellicott City, MD, USA  
e-mail: nichols@mirc-us.com

© Springer International Publishing AG, part of Springer Nature 2019

L. D. Wright and C. R. Nichols (eds.), *Tomorrow's Coasts:*

*Complex and Impermanent*, Coastal Research Library 27,

[https://doi.org/10.1007/978-3-319-75453-6\\_7](https://doi.org/10.1007/978-3-319-75453-6_7)

bring storm surges along with heavy rainfall and wave induced set up of mean water level. Structures such as levees that are designed to protect can also impede the return of floodwaters once overtopped. Navigation channels can also provide funneling pathways for surges.

In addition to extensive loss of life, there are many other negative consequences of coastal inundation. Some of the more obvious impacts include destruction of houses and buildings and damage to built infrastructure such as roads and bridges. Less visible are mold infestations inside homes that are flooded but not destroyed. Floodwaters can be contaminated with sewage and lingering inundation can spread diseases throughout neighborhoods and contaminate drinking water. Salt water can penetrate into aquifers and ground water and high salinities can kill vegetation and degrade wetlands. In some cases, severely inundated communities may be forced to relocate. Details of the human health impacts of coastal inundation are presented in Chap. 10.

## 7.2 Tsunamis

Sea floor seismic events such as earthquakes, volcanic activity and underwater landslides that cause sudden and large displacements of the overlying water column are the cause of tsunamis (previously called tidal waves). The vertically displaced water creates a long gravity wave that then travels away from the area of disturbance at speeds that are proportional to the square root of the water depth. In the deep ocean these speeds may exceed 500 mi/h (800 km/h). The wave is not a single wave but a train of multiple succeeding waves separated by distances (wave lengths) of 300–400 km (190–250 mi) and time intervals (periods) of 30–40 min. In the deep ocean, the heights of the tsunamis are typically on the order of 1 m or less (<3.3 ft) and so this rise over the large horizontal distance (wave length) and time interval (period) makes these waves imperceptible to ships at sea. However, as the tsunami propagates into the shallow waters over the continental shelf, their speeds and wavelengths decrease dramatically while their periods remain constant. The energy that was previously distributed over a very large horizontal distance now becomes more concentrated and the tsunami undergoes what is generally referred to as a shoaling amplification that causes the tsunami height to increase many times relative to its deep ocean height.

The Asian tsunami of December 26, 2004 (NOAA/NGDC 2014; Pomonis et al. 2006; Titov et al. 2005), that killed 230,000 people and caused \$10 billion (USD) in damages originated from a seafloor seismic disturbance at a depth of ~4000 m (13,000 ft), had a deep sea amplitude of 70 cm (2.3 ft) and initially travelled away from the epicenter at a speed of 720 km/h (450 mi/h). It had a period of 34 min and a deep-water wavelength of 410 km (256 mi). By the time it reached nearshore depths of 5 m (17 ft) its length would have decreased to about 14 km (8.75 mi).

Because of the complex configuration of the shelf and coast around the area of greatest devastation in Indonesia and Thailand the height of the “wall of water” that made landfall varied considerably but exceeded 10 m (33 ft) in places of greatest impact. The magnitude 9 Tohoku earthquake (Dunbar et al. 2011) that occurred east of Honshu Island Japan on March 11, 2011 generated a 15 m (50 ft) tsunami that devastated Fukushima Japan, killed 19,000 people and inundated a nuclear power plant. Since the epicenter was adjacent to the coast, the arrival of the tsunami was immediate with minimal warning. Following the impact on Japan, the wave crossed the Pacific Ocean at speeds proportional to the square root of the abyssal water depths as shown in Fig. 7.1. Note from Fig. 7.1 that the tsunami reached southern California about 10 h after the earthquake, roughly about the same as the time required for a jet liner to make the same trip.

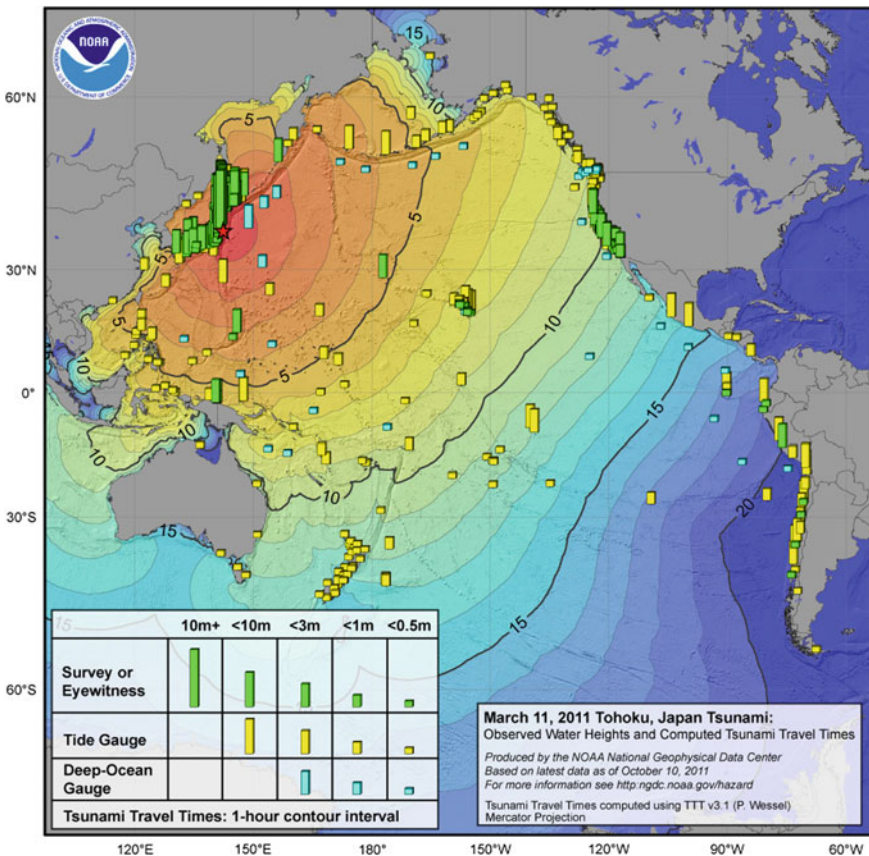


**Fig. 7.1** Observed heights and travel times of the Tohoku Tsunami that devastated Fukushima Japan in March, 2011. Graphic from the NOAA National Geophysical Data Center

### 7.3 Storm Surges and Storm Tides

Storm surges are elevated water levels near the coast primarily caused by severe atmospheric disturbances such as tropical storms and hurricanes as well as less severe storms such as mid latitude “northeasters”, all of which involve strong winds. Dean and Dalrymple (2002) describe four major components that jointly contribute to storm surges. The most important of these factors is wind stress (or frictional force) of the wind blowing over the sea surface and pushing the water shoreward. Added to this is the secondary “inverse barometer” effect whereby low barometric pressure causes a rise in the water level below (or “barometric tide”; Dean and Dalrymple 2002). Typically, this effect accounts for only about 5% of the total surge height. A third component is the Coriolis force related to the earth’s rotation, which, causes water to be deflected to the right in the northern hemisphere and to the left in the southern hemisphere. In the northern hemisphere, this results in south-flowing currents on east coasts and north-flowing currents on west coasts (such the Florida Gulf Coast) causing rises in water levels at the shore and near shore. The fourth component is a water level “setup” caused by the dissipation of breaking waves (surf) and is often equal to 10% or more of the breaker heights themselves. The storm waves are then superimposed on this surge and can reach much farther inland than would be the case without the surge. *Storm tides*, as distinct from storm surges, are the water levels that result from the addition of normal astronomical tide levels and the superimposed storm surges. The total impact of a storm surge coinciding with a high tide, particularly a perigean spring tide (“King tide”) will be much greater than if the predicted tide is low at the time the storm surge reaches its maximum.

The magnitudes of the four main components of storm surges as introduced above provide an approximate basis for quantifying the heights of storm surges at the coast. Unlike tsunamis- and tides- storm surges are not freely propagating waves emanating from a source off the coast. Instead, these waves are locally forced (Resio and Westerink 2008). Consequently, surges are not strongly affected by processes such as refraction and shoaling. As shown by Resio and Westerink (2008), primary factors affecting surges depend strongly on the wind speed, the width and slope of the continental shelf and on the configuration and irregularity of the shores, bays and crenulations that can amplify or diminish the surge. Given the same forcing, the largest surges are generated over wide, shallow and gently sloping shelves and the smallest would be generated over narrow, steep shelves. For example, the storm surge that Category-5 Hurricane Andrew generated in Miami, which is fronted by a steep and very narrow shelf, was less than 2 m (6.6 ft) high in most places although it reached 5 m (16.4 ft) in parts of Biscayne Bay (Rappaport 1993). In contrast, an 8.5 m (28 ft) surge was generated by the weaker, but much larger Hurricane Katrina over the shallow shelf of the northern Gulf of Mexico in 2005. Some of the greatest amplification of surges can be affected significantly by alongshore processes when the surge “wave” propagates along the coast at roughly the same speed as the surge-generating storm advances. It is primarily because of

the wide, shallow shelves that front the U.S. Atlantic and Gulf coasts that storm surges are much more consequential there than they are on the Pacific Coast. In addition to surge amplification by propagation across wide continental shelves, other amplification processes may operate. Among these, are amplification of surges travelling up funnel-shaped bays or estuaries and resonant seiche within some harbors or bays.

The operational storm surge prediction model used by NOAA's National Weather Service (NWS) is the 2-dimensional *Sea, Lake and Overland Surges from Hurricanes (SLOSH)* model (Jelesnianski et al. 1992). Even though there are numerous more sophisticated and accurate models available and used by academia and other federal agencies (described in Chap. 1), SLOSH continues to be preferred by the NWS because of its speed of execution and low computational requirements and because forecasters are familiar with it. For purposes of long-range emergency planning, assessing evacuation routes and assessing relative risk of flooding of specific localities, NOAA's National Hurricane Center runs SLOSH thousands of times for different hypothetical hurricanes to generate vulnerability maps of worse case scenarios of flooding. These maps portray the quantities *Maximum Envelopes of Water (MEOW)* and the *Maximum of MEOWs (MOM)*. Figure 7.2 shows a map of MOMs for hypothetical Category 3 hurricanes hitting the southern part of the Florida peninsula. Note that predicted inundation maxima along the open coast, neglecting wave setup, are fairly minimal for the Miami area and southeast Florida where the shelf is very narrow and steep but exceeds 2.7 m (9 ft) on the western side where a wide, low gradient shelf prevails (see Fig. 14.2 in Chap. 14). It should be noted that a Category 3 hurricane is not really extreme over decadal time frames. Consequently, the surge heights predicted by FEMA to have a statistical 100-year return interval are larger than those shown in Fig. 7.2. Although the predicted surge heights on the Atlantic side are low, flooding by wave-induced setup and runup may be greater but surf effects are not included in these analyses.

An interesting comparison between Hurricanes Camille in 1969 and Katrina in 2005 shows the inherent importance of hurricane size on storm surges at the coast. Camille was a Saffir-Simpson category 5 hurricane when it struck the Mississippi coast, while Katrina was only a category 3 hurricane when it reached this coast. Because of this, many people underestimated the potential danger of Katrina and chose not to evacuate. As noted by Irish et al. (2008), an article on the rising death toll in Hurricane Katrina found in Biloxi, Mississippi's Sun Herald (Norman 2006), "an oft heard refrain ... is Hurricane Camille killed more people in 2005 than it did in 1969. Many officials and locals believed those ... who had survived what was then the strongest recorded hurricane were lulled into a false sense of security that kept them in harm's way."

Even today, many people still echo the sentiment that it would have been much worse if a Saffir-Simpson category 5 storm had struck this area rather than Katrina. Irish et al. (2008) developed evidence showing that the Saffir-Simpson scale is not a particularly good indicator of storm surge along the coast and that storm size, along with bottom slope, is also a critical factor in the generation of large coastal surges. Figure 7.3 shows a plot of the surge contours for an idealized 1:10,000

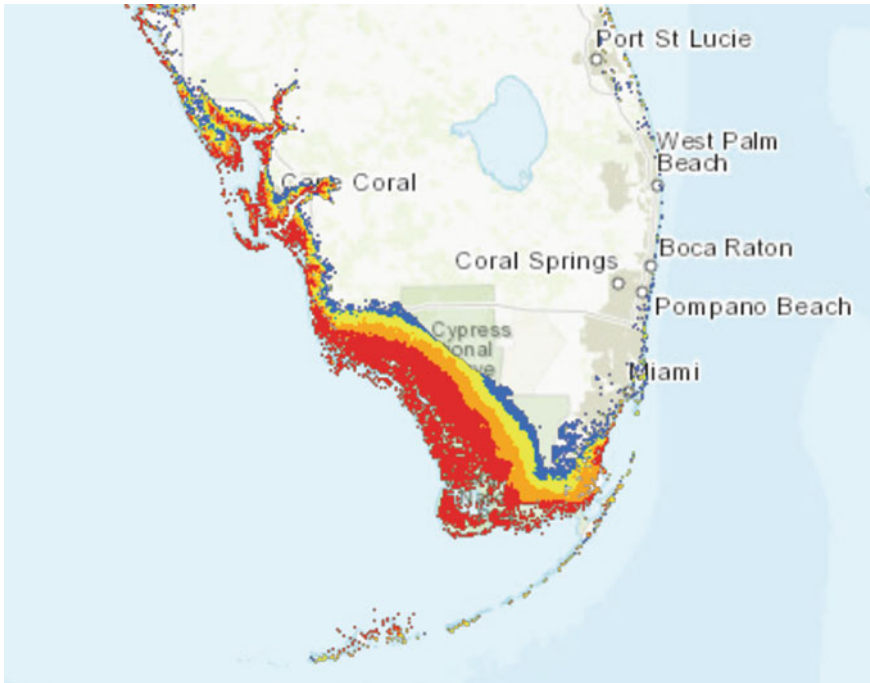


**Fig. 7.2** Predicted maxima of maximum envelope of water (MOMs) for a category 3 Hurricane affecting south Florida. Red=greater than 9 ft (2.7 m) above ground; Orange=greater than 6 ft (1.8 m) above ground; yellow=greater than 3 ft (0.9 m) above ground; blue= less than 3 ft (0.9 m) above ground *Source* NOAA/NWS/NHC/Storm Surge Unit, NOAA/NOS/Office for Coastal Management. <http://noaa.maps.arcgis.com/apps/MapSeries/index.html?appid=d9ed7904dbec441a9c4d7b277935fad&entry=1>

slope, generated by computer simulations with the ADICRC code. Different symbols superimposed on the contours represent estimates of potential surge heights for historical hurricanes in the Gulf of Mexico. As can be seen in this figure, and consistent with actual surge heights, the surge generated by Katrina was significantly larger than that of Camille. In simple terms, larger storms generate higher surges.

#### 7.4 Wave-Induced Setup, Runup and Overtopping

In the foregoing discussion on storm surge, we noted that, according to Dean and Dalrymple (2002) one of the four components of storm surge, as manifest at the shore is *wave setup* (Stockton et al. 2005; FEMA 2015; Fig. 7.4). In fact, this setup represents the transfer of momentum from the wave field into the mean current flow, which occurs when waves break and dissipate. The setup elevation can be



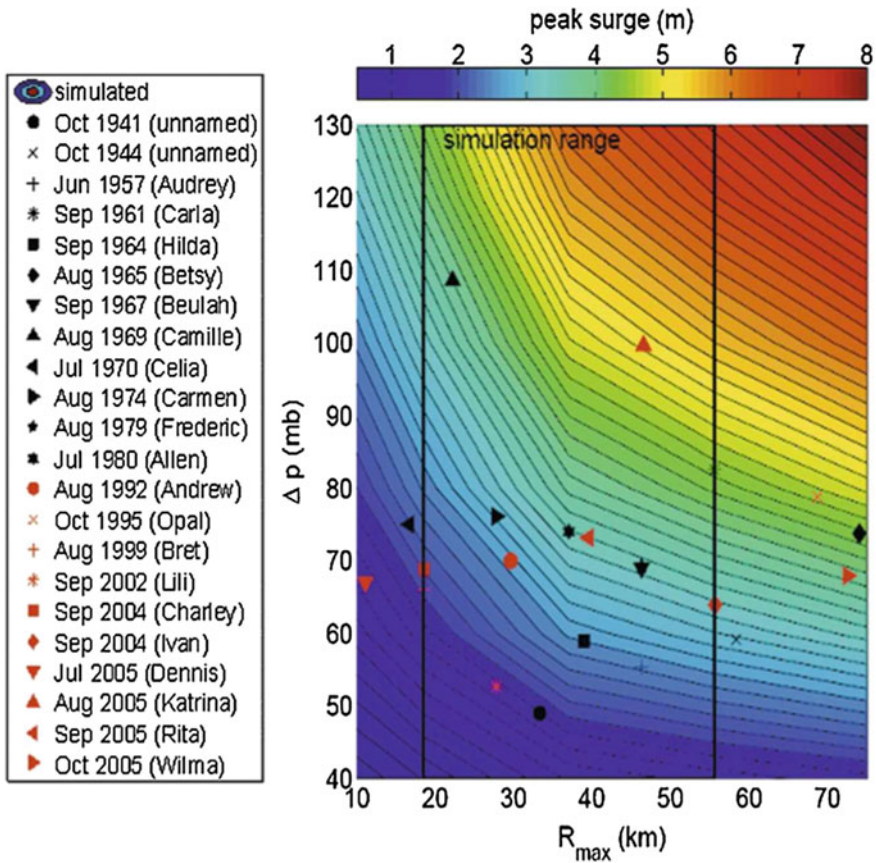


**Fig. 7.3** Simulated peak surge as a function of hurricane size (denoted here by the radius to maximum winds,  $R_{max}$ ) and intensity (taken as the pressure differential from the center of the storm to its periphery,  $\Delta p$ ) for a 1:10,000 bottom slope. Historical size and central pressure observations are superimposed on the numerical results to indicate the potential peak surge potential of historical storms made landfall in a region characterized by a bottom slope of 1:10,000, which is similar to the Mississippi Gulf Coast

10%- 20% of the height of the waves breaking in nearshore areas (FEMA 2015). Because breaking waves commonly arrive in varying “packets” of high and low waves, the setup height is not constant but usually forces “infragravity” periods of 50–100 s, traditionally called “surf beat” along many swell-dominated coasts (Guza and Thornton 1985). After transiting the surf zone, waves that have not been fully dissipated then surge up and down a beach or coastal engineering structure as *wave runup* the height of which increases with wave height and length and with beach slope (Fig. 7.5; Mignone and Maine 2016; Jones et al. 2005; Senechal et al. 2011). *Overtopping* occurs when the height of runup exceeds the height of the beach berm,

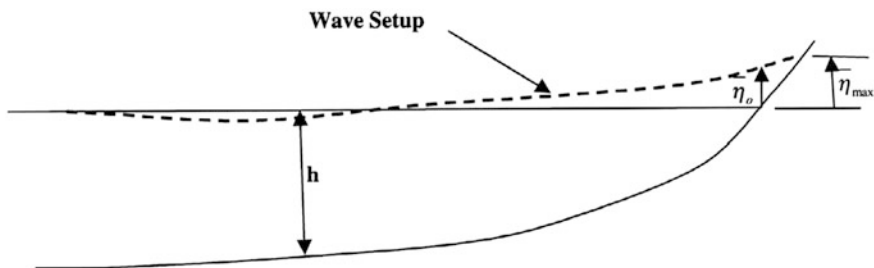


**Fig. 7.4** Wave setup is a rise in the mean water level within the surf zone and on the beach caused by the dissipation that accompanies wave breaking. Diagram is from FEMA (2015), Guidance document 44 for the simple case of monochromatic waves

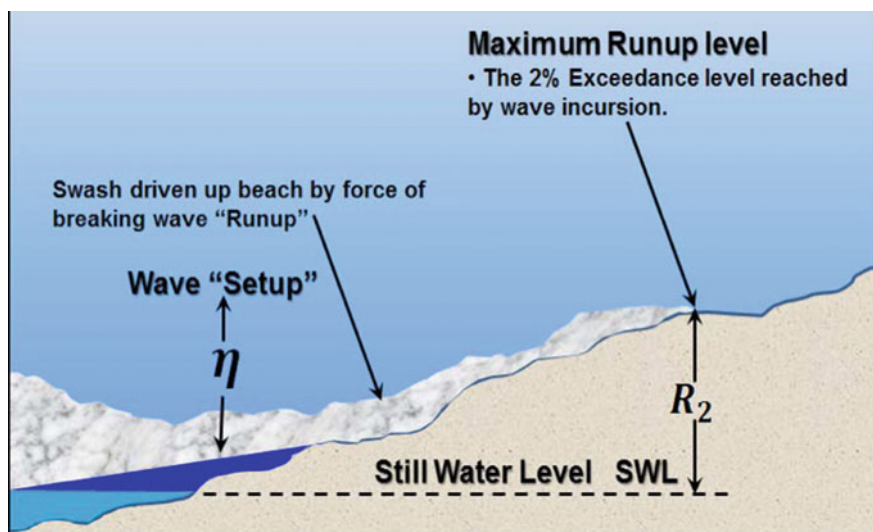


**Fig. 7.5** Wave runup is superimposed on wave setup and reaches higher up the beach than setup. Figure from Mignone (2016), NOAA, National Weather Service, based on the model of Stockton et al. (2005)

protective dune or seawall and can result in flooded roadways or land surfaces (Fig. 7.6).

While the largest storm surges occur on coasts fronted by wide, gently sloping shelves, the heights and impacts of wave setup, runup and overtopping are greater on the more exposed shores fronted by steep and narrow shelves which favor high breakers because of less attenuation. It is in fact fortunate that the regimes that favor the highest surf do not also favor the highest storm surges. As is indicated by Fig. 7.2, the Atlantic coast of south Florida is much less vulnerable to storm surge than is Florida’s Gulf Coast but the surf-related inundation is much greater for Miami-Dade and Broward Counties. And this was the case for the entire Atlantic





**Fig. 7.6** Splash-over and wave overtopping at Crescent Beach in the Town of Hull, MA during the Patriot’s Day Storm of 2007. High winds, heavy rainfall, and high tides during this nor’easter caused flooding, storm damages, power outages, evacuations, and disrupted traffic and commerce (photo from Applied Coastal Research and Engineering, Inc. 2015)

seaboard as Hurricane/Superstorm Sandy moved northward in 2012. With specific reference to Sandy, Mignone and Maine (2016) reports that: “NWS (National Weather Service) lacks sufficient forecast guidance on inundation associated with wave runup and coastal rivers making it difficult to forecast impacts from coastal storms”. This points to the urgent need to couple storm surge, nearshore (surf zone) and hydrology models for future forecasting capabilities.

## **7.5 Minor, but Frequent, Coastal Flooding (a.k.a. “Nuisance Flooding”)**

Severe events such as tsunamis and tropical cyclones are the causes of the most dangerous and damaging inundation. However, important problems in many areas are associated with much smaller, much more frequent events, which can produce recurrent and problematic flooding even under fair weather conditions. Rising sea levels and subsiding land levels make their presence felt in troublesome ways during times of high, but normal, astronomical tides. On coasts where land surfaces rise abruptly with distance from the sea, these effects may be minimal. But in other cases where land elevations rise slowly or where urban and suburban areas are near or even below mean sea level, high tides are increasingly accompanied by shallow, but sometimes paralyzing, flooding of streets, neighborhoods and occasionally the

ground floors of homes and buildings. NOAA (Sweet et al. 2014) refers to these situations as “nuisance flooding”. The threshold for an excess water level rise to be a nuisance varies with location depending primarily on surface elevation and secondarily on several other factors including socioeconomic vulnerability, and public infrastructure including roads and storm water drainage.

As we might expect, given local topography, in the U.S. the threshold is fairly high on the generally higher and steeper west coast and lower (more troublesome) on the Atlantic and Gulf coasts (Sweet et al. 2014). The Atlantic and Gulf coasts are low lying and, for the most part, experiencing significant subsidence. On the U.S. Atlantic coast, the aperiodic variations in sea level are related to occurrences of strong onshore winds as well as fluctuations in the flow of the Gulf Stream (Ezer 2013; Ezer and Atkinson 2014; see Chap. 3, Sect. 3.5; Chap. 14). Tide ranges also vary somewhat over the course of a year and are greatest during perigean tides when the earth and moon are closest (e.g. at times of “harvest moons” in October). Perigean spring tides are locally referred to as “King Tides” because the range is above normal. King tides alone do not constitute nuisance flooding. But it is when higher sea levels combine with onshore winds and effects related to the slackening of the Gulf Stream that these nuisances happen. Since sea levels are progressively rising, the frequency of occurrence of nuisance floods is increasing and when torrential rainfalls and clogged storm drains coincide with nuisance flood events, the effects sometimes become somewhat more than a nuisance (Sweet et al. 2014). As shown in Fig. 7.7, the number of days with nuisance flooding in Atlantic City, New Jersey have steadily increased from 0 to 5 days per year in the 1950s to over 30 days in 2012. Similar trends are evident at other U.S. Atlantic and Gulf Coast locations.

## 7.6 Compound Ocean, Fluvial and Pluvial Flooding

Considerations of coastal flooding tend to place heavy emphasis on storm surge and model predictions of inland flooding during tropical cyclones produced by storm surge models, such as SLOSH, as described in subsection 7.3. Storm surges are, of course, a major concern but their effects are increasingly magnified by those of less

**Fig. 7.7** Graph and scatter plot showing the number of days per year with nuisance flooding at Atlantic City, New Jersey from 1920 to the present based on NOAA tide gage records. From Sweet et al. (2014, NOAA Technical Report NOS CO-OPS 073)

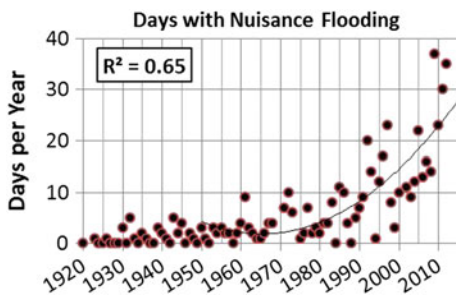




**Fig. 7.8** Aerial image of a pluvial flood in Louisiana in 2016. Image created using data collected by National Oceanic and Atmospheric Administration for the National Geodetic Survey. *Credit* Jason Burton/USGS. From Witman (2017)

well predicted phenomena such river, or fluvial, flooding and pluvial flooding (Fig. 7.8) by extreme and often unexpected torrential and prolonged rainfall. If the ground is already saturated from previous rains, the effects can be further exacerbated. When all three, or even two, of these inundation phenomena coincide, the compound effects can be catastrophic as was recently demonstrated when Hurricane Harvey made landfall on the coast of Texas and caused widespread flooding of Houston in late August, 2017. The coasts of south Asia are subject to compound flooding on a near annual basis. As explained in Chap. 2, flooding of the Ganges-Brahmaputra delta, home to 200 million people, is caused by the combination of storm surge, river flooding and torrential rain during the summer monsoon season. In Guangzhou, China and the Pearl River delta, severe rainstorms, which may or may not accompany typhoons are responsible for 63% of the flood-related economic losses while storm surges caused by typhoons directly account for 33% (He and Yang 2011; Chap. 12). Lian et al. (2013) describe the increase of similar threats from compound flooding in Fuzhou, China, with the greatest threat attributable to heavy rainfall.

Wahl et al. (2015) have examined the joint probability of severe storm surge and pluvial flooding coinciding in U.S. coastal cities and concluded that the occurrence of such compound events has increased significantly over the past century. Ikeuchi et al. (2017) have developed a large-scale global coupled river-coast flood model. Their results indicate that the greatest risks from compound flooding are in mega-deltas, particularly the large Asian deltas, and estuaries where storm surges can propagate over 200 km (124 mile) upstream. A crucial aspect of compound floods is that the storm surge not only contributes its own component of inundation,

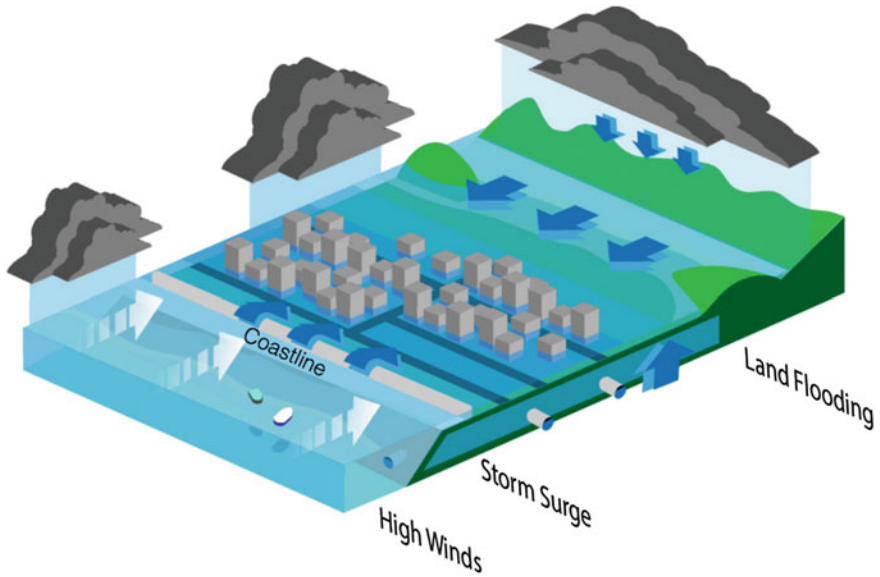


**Fig. 7.9** The joint occurrence of torrential rainfall and storm surge causes compound flooding in coastal regions because storm surge not only causes inundation but also slows or blocks freshwater drainage. From Wahl and Jains (2015). How storm surges and heavy rainfall drive coastal flood risk in the U.S. *Carbon Brief* 27 July 2015. *Diagram Credit* Theodore Scontras, University of Maine

it also opposes the drainage of the pluvial floodwaters from the land. This is illustrated conceptually in Fig. 7.9. Reed et al. (2015) conclude that the risk of such compound flooding in New York City is increasing.

High sea surface temperatures fuel tropical cyclones in several ways. Most importantly they favor rapid storm intensification and increased amounts of rainfall and in combination, these factors can lead to compound flooding. As it traversed the northern Gulf of Mexico *en route* to eventual landfall on the east Texas coast, Hurricane Harvey was nourished by sea surface temperatures in excess of 30 °C (85 °F). Then, prior to landfall it encountered an eddy consisting of even warmer water and, overnight, it intensified from a depression to a hurricane (Fischetti 2017) and incorporated excessive amounts of water vapor into its core before making landfall as a Category 4 Hurricane and then stalling a short distance inland. Although the storm surge generated by Harvey was fairly modest in most places, the rainfall was extreme: peak accumulations reached 64.58 in (164.0 cm) making Harvey the wettest tropical cyclone to ever hit the U.S. Flooding of Houston was uncommonly widespread and prolonged. As discussed in Part 1, Chap. 2, rising ocean temperatures are likely to increase the severity, but not necessarily the frequency, of future such events.

## 7.7 Flood Mitigation, Storm Water Drainage and Runoff

Extensive engineering works to protect cities and communities from floods have been constructed in many developed countries, particularly in Europe. As pointed out in Chap. 6, the low-lying Netherlands has been a world leader in coastal engineering for many decades. A complex system of dunes, dikes, floodgates and frequent land reclamation maintains lands that would be frequently or continually submerged. Subsequent to the devastation caused by Hurricane Katrina, the U.S. Army Corps of Engineers has completed a \$14.5B flood protection system intended to withstand a 100-year flood event. This system consists of levees, a 26ft (8 m) high storm surge barrier and high-volume pumps (Fig. 7.10; Burnett 2015). According to the Southeast Louisiana Flood Protection Authority, the pumping system is the largest in the world and can fill an Olympic size swimming pool in 3 s. But despite its cost and size, the system still does not meet the design criteria specified by Congress in 1965 and New Orleans continues to be threatened. And chronic failures of the system occurred in summer, 2017.

Following the lessons that New York learned from Hurricane Sandy, plans are underway to surround lower Manhattan with a ten-foot (3 m) high wall extending from the end of E. 42nd St. to W. 57th St. at a cost of more than US \$3 billion (Goodell 2017).

It is often easier to predict the level of coastal inundation by storm surge than it is to predict how long it will take for floodwaters to subside. This is because there

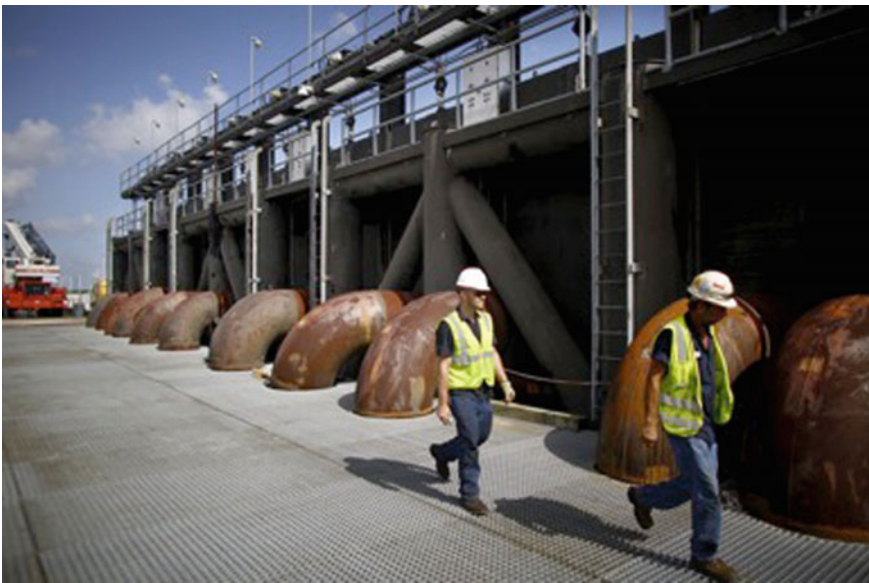


**Fig. 7.10** Storm surge barrier and pumping pipes at the 17th Street Canal in New Orleans (photo by David Gilkey/NPR)



are numerous natural and anthropogenic factors that control storm water drainage and runoff. Natural factors include the degree to which the ground is already saturated, whether or not the wind blows from a direction that opposes runoff, local topography and the stage levels and proximity of local river and streams. Human factors include the extent of paved surfaces, the effectiveness of drainage systems, engineered flood control systems such as pumps and—perhaps most difficult of all—how managers triage decisions regarding the opening or closing of flood control dams and floodgates. For example, decisions by the U.S. Army Corps of Engineers concerning where and when to relieve the rising waters of the Mississippi River flood of 1927 were beneficial for some and devastating-and fatal- for others (Barry 1997).

## 7.8 The Road Ahead for Flood Mitigation

Goodell (2017) in his popular book *The Water Will Come*, discusses changing climate, increasing coastal populations, and significant flood damage that is occurring worldwide. He provides illustrations of flooding in Miami-Dade County, where inundation and sewer overflows are attributed to sea level rise and the conversion of pervious surfaces into impervious (i.e. paved) surfaces, result in increased volumes of runoff which exceed the capacity of sewer systems. Major coastal construction efforts are planned to combat sea level rise and sinking cities such as Venice, the capital of northern Italy's Veneto region, is a prime example. Venice, which is reportedly subsiding approximately 1–2 mm per year (0.04–0.08 in. per year), was built on small islands in the Adriatic Sea (e.g., Bock et al. 2012; Tosi et al. 2015). Complex structures and solutions to protect Venice include installation of mobile barriers in the lagoon that will lie on the sea floor, but inflate during high tides. Perhaps the most ambitious and futuristic proposal would involve injection of billions of gallons of seawater into porous sediments under the canal-crossed city, to raise the city (e.g., Comerlati et al. 2004; Teatini et al. 2010). Other options include retreat, which involves no effort to protect the land from rising sea levels and inundation. This implies acceptance of the reality that people will not prevent the land from flooding, but must adapt by erecting emergency flood shelters, elevating buildings, or moving structures inland.

## References

- Applied Coastal Research and Engineering, Inc. 2015, June 30. Environmental notification form: Crescent beach seawall and revetment repair hull. 38pp, plus appendices. Prepared for Town of Hull Conservation Department.
- Barry, J.M. 1997. *Rising tide: The great Mississippi flood of 1927 and how it changed America*, 524. New York: Touchstone.



- Bock, Yehuda, Shimon Wdowinski, Alessandro Ferretti, Fabrizio Novali, and Alfio Fumagalli. 2012. Recent subsidence of the Venice lagoon from continuous GPS and interferometric synthetic aperture radar. *Geochemistry, Geophysics, Geosystems* 13 (3): 1–13. <https://doi.org/10.1029/2011GC003976>.
- Burnett, John. 2015, Aug 28. Billions spent on flood barriers, but New Orleans still a ‘fishbowl’. *NPR*. Available online <http://www.npr.org/2015/08/28/432059261/billions-spent-on-flood-barriers-but-new-orleans-still-a-fishbowl>. Accessed on 25 Sept 2017.
- Comerlati, Andrea, Massimiliano Ferronato, Giuseppe Gambolati, Mario Putti, and Pietro Teatini. 2004. Saving Venice by seawater. *Journal of Geophysical Research: Earth Surface* 109 (F3): F03006. <https://doi.org/10.1029/2004JF000119>.
- Dean, R.G., and Dalrymple R.A. 2002. *Coastal processes with engineering applications*. Cambridge University Press. 475pp.
- Dunbar, P., H. McCullough, G. Mungov, J. Varner, and K. Stroker. 2011. 2011 Tohoku earthquake and tsunami data available from the national oceanic and atmospheric administration/national geophysical data center. *Geomatics, Natural Hazards and Risk* 2 (4). <https://doi.org/10.1080/19475705.2011.632443>.
- Ezer, T. 2013. Sea level rise, spatially uneven and temporally unsteady: Why the U.S. East Coast, the global tide gauge record, and the global altimeter data show different trends. *Geophysical Research Letters* 40 (20): 5439–5444. <https://doi.org/10.1002/2013GL057952>.
- Ezer, T., and L.P. Atkinson. 2014. Accelerated flooding along the U.S. East Coast: On the impact of sea-level rise, tides, storms, the Gulf Stream, and the North Atlantic Oscillations. *Earth's Future* 2 (8): 362–382. <https://doi.org/10.1002/2014EF000252>.
- FEMA. 2015. *Guidance for flood risk analysis and mapping. Coastal wave setup*. Guidance document 44.
- Fischetti, M. 2017. Hurricane Harvey: Why is it so extreme? *Scientific American*. 28 Aug 2017.
- Goodell, J. 2017. *The water will come*, 340. New York, NY: Little Brown and Company.
- Guza, R.T., and E.B. Thornton. 1985. Observations of surf beat. *Journal Geophysical Research* 90: 361.
- He, C., and L. Yang. 2011. Urban development and climate change in China’s Pearl River delta. *Land Lines*. Lincoln Institute of Land Policy. 7pp.
- Ikeuchi, H., Y. Hirabayashi, D. Yamazaki, S. Muis, P.J. Ward, H.C. Winsemius, M. Verlaan, and S. Kanae. 2017. Compound simulation of fluvial floods and storm surges in a global coupled river-coast flood model: Model development and its application to 2007 Cyclone Sidr in Bangladesh. *Journal of Advances in Modeling Earth Systems* 9: 1847–1862. <https://doi.org/10.1002/2017MS000943>.
- Irish, J.L., D.T. Resio, and J.J. Ratcliff. 2008. The influence of storm size on hurricane surge. *Journal of Physical Oceanography* 38 (11): 2003–2013.
- Jelesnianski, C.P., J. Chen, and W.A. Shaffer. 1992. *SLOSH: Sea, lake, and overland surges from hurricanes*. NOAA Technical Report NWS 48. Silver Spring, MD: National Weather Service, NOAA. 77pp.
- Jones, C., et al. 2005. Wave runup and overtopping. In *FEMA coastal flood hazard analysis and mapping guidelines: Focused study report*.
- Lian, J.J., K. Xu, and C. Ma. 2013. Joint impact of rainfall and tidal level on flood risk in a coastal city with a complex river network: A case study of Fuzhou City, China. *Hydrology and Earth System Sciences* 17: 679–689. <https://doi.org/10.5194/hess-17-679-2013>.
- Mignone, A., and Caribou Maine. 2016. *Forecasting wave runup and overtopping*. National Weather Service VLabForum.
- NOAA National Geophysical Data Center (NGDC). 2014. Tsunami Event Database. <http://www.ngdc.noaa.gov/nndc/struts/form?t=101650&s=70&d=7>.
- Norman, J. 2006. Katrina’s dead. *Sun Herald* A1, A8–9. 17 Feb 2006.
- Pomonis, A., T. Rossetto, N. Peiris, S. Wilkinson, D. Del Re, R. Koo, R. Manlapig, and S. Gallocher. 2006. *The Indian ocean tsunami of 26 December 2004: Mission findings in Sri Lanka and Thailand*, 180. London, UK: Technical Report of Earthquake Engineering Field Investigation Team.

- Rappaport, E. 1993. *Preliminary report Hurricane Andrew 16–28 August 1992*. National Center for Environmental Prediction (NCEP) Technical Report.
- Reed, A.J., et al. 2015. Increased threat of tropical cyclones and coastal flooding to New York city during the anthropogenic era. *Proceedings of the National Academy of Sciences*. <https://doi.org/10.1073/pnas.1513127112>.
- Resio, D.T., and J.J. Westerink. 2008. Modeling the physics of storm surges. *Physics Today* 61: 33.
- Senechal, N., G. Coco, K.R. Bryan, and R.A. Holman. 2011. Wave runup during extreme storm conditions. *Journal Geophysical Research* 116: C07032. <https://doi.org/10.1029/2010JC006819>.
- Stockton, H., R.A. Holman, P. Howd, and A.H. Sallenger Jr. 2005. Empirical parameterization of setup, swash, and runup. *Coastal Engineering* 53 (7): 573–588. <https://doi.org/10.1016/j.coastaleng.2005.12.005>.
- Sweet, W., J. Park, J. Marra, C. Zervas, and S. Gill. 2014. Sea level rise and nuisance flood frequency changes around the United States. NOAA Technical Report NOS CO-OPS 073. 58pp.
- Teatini, Pietro, Massimiliano Ferronato, Giuseppe Gambolati, D. Baù, and Mario Putti. 2010. Anthropogenic Venice uplift by seawater pumping into a heterogeneous aquifer system. *Water Resources Research* 46 (11): W11547. <https://doi.org/10.1029/2010wr009161>.
- Titov, V.V., A.B. Rabinovich, H.O. Mofjeld, R.E. Thomson, and F.I. González. 2005. The global reach of the 26 December 2004 Sumatra Tsunami. *Science* 309 (5743): 2045–2048.
- Tosi, Luigi, Tazio Strozzi, Cristina Da Lio, and Pietro Teatini. 2015. Regional and local land subsidence at the Venice coastland by TerraSAR-X PSI. *Proceedings of the International Association of Hydrological Sciences* 372: 199–205. <https://doi.org/10.5194/piahs-372-199-2015>.
- Wahl, T., and S. Jain. 2015. How storm surges and heavy rainfall drive flood risk in the U.S. *Carbon Brief* 27 July 2015. <https://www.carbonbrief.org/how-storm-surges-and-heavy-rainfall-drive-coastal-flood-risk-in-the-us>.
- Wahl, T., S. Jain, et al. 2015. Increasing risk of compound flooding from storm surge and rainfall for major US cities. *Nature Climate Change*. <https://doi.org/10.1038/nclimate2736>.
- Witman, S. 2017. Deciphering deluges. *EOS* 98 (11): 42.